10-1-2016

Chronic expression of interferon-gamma leads to murine autoimmune cholangitis with a female predominance

Heekyong R. Bae
National Cancer Institute at Frederick

Patrick S.C. Leung
UC Davis School of Medicine

Koichi Tsuneyama
Tokushima University

Julio C. Valencia
National Cancer Institute at Frederick

Deborah L. Hodge
National Cancer Institute at Frederick

See next page for additional authors

HEPATOLOGY

HEPATOLOGY, VOL. 64, NO. 4, 2016

Chronic Expression of Interferon-Gamma Leads to Murine Autoimmune Cholangitis With a Female Predominance

Heekyong R. Bae,[1] Patrick S.C. Leung,[2] Koichi Tsuneyama,[3] Julio C. Valencia,[1] Deborah L. Hodge,[1] Seohyun Kim,[1] Tim Back,[1] Megan Karwan,[4] Anand S. Merchant,[5] Nobuyuki Baba,[6] Dechun Feng,[7] Ogyi Park,[8] Bin Gao,[7] Guo-Xiang Yang,[2] M. Eric Gershwin,[2] and Howard A. Young[1]

In most autoimmune diseases the serologic hallmarks of disease precede clinical pathology by years. Therefore, the use of animal models in defining early disease events becomes critical. We took advantage of a "designer" mouse with dysregulation of interferon gamma (IFNγ) characterized by prolonged and chronic expression of IFNγ through deletion of the IFNγ 3′-untranslated region adenylate uridylate-rich element (ARE). The ARE-Del$^{-/-}$ mice develop primary biliary cholangitis (PBC) with a female predominance that mimics human PBC that is characterized by up-regulation of total bile acids, spontaneous production of anti-mitochondrial antibodies, and portal duct inflammation. Transfer of CD4 T cells from ARE-Del$^{-/-}$ to B6/Rag1$^{-/-}$ mice induced moderate portal inflammation and parenchymal inflammation, and RNA sequencing of liver gene expression revealed that up-regulated genes potentially define early stages of cholangitis. Interestingly, up-regulated genes specifically overlap with the gene expression signature of biliary epithelial cells in PBC, implying that IFNγ may play a pathogenic role in biliary epithelial cells in the initiation stage of PBC. Moreover, differentially expressed genes in female mice have stronger type 1 and type 2 IFN signaling and lymphocyte-mediated immune responses and thus may drive the female bias of the disease. *Conclusion:* Changes in IFNγ expression are critical for the pathogenesis of PBC. (HEPATOLOGY 2016;64:1189-1201)

SEE EDITORIAL ON PAGE 1024

As with most autoimmune diseases, primary biliary cholangitis (PBC) is female-predominant and has a long latency period between detection of autoantibodies and the clinical appearance of immunopathology.[1-4] Although there are clearly major defects in adaptive immunity, including dysregulation of multiple T-cell and B-cell pathways,[5-11] there is significant evidence for the role of innate immunity in modulating and perhaps even initiating disease activity.[12-17] Indeed, we have proposed that PBC is a multihit disease involving independent but overlapping immune pathways that interact at different stages of disease activity, ultimately leading to the clinical entity of severe portal inflammation with potential cirrhosis.

The role of interferon (IFN) in autoimmunity is controversial, but a T-helper 1 (Th1) cell-mediated inflammatory response appears critical for loss of tolerance. In the present study, we took advantage of a mouse in which there is a deletion of the IFN 3′-untranslated region adenylate uridylate-rich element, resulting in chronic IFN expression, and report here that these mice not only develop the classic histologic features of autoimmune cholangitis but, more importantly, have a gender-differential bias as well as characteristic dysregulation of bile acids. We propose that

Abbreviations: AMA, anti-mitochondrial antibodies; BCOADC-E2, branched chain 2-oxo-acid dehydrogenase E2 subunit; BEC, biliary epithelial cell; GWAS, genome-wide association study; H&E, hematoxylin and eosin; IFN, interferon; IL, interleukin; IPA, Ingenuity Pathway Analysis; MCP-1, monocyte chemoattractant protein-1; MHC, major histocompatibility complex; OGDC-E2, 2-oxo-glutarate dehydrogenase E2 subunit; PBC, primary biliary cholangitis; PDC-E2, pyruvate dehydrogenase complex E2 subunit; TBA, total bile acids; Th1, T-helper 1; TNF, tumor necrosis factor.

Received March 15, 2016; accepted April 28, 2016.

Additional Supporting Information may be found at onlinelibrary.wiley.com/doi/10.1002/hep.28641/suppinfo.

Supported in part by National Institutes of Health grant DK090019 (to M.E.G.).

View this article online at wileyonlinelibrary.com.

DOI 10.1002/hep.28641

Potential conflict of interest: Nothing to report.

IFN dysregulation leads to initiation of PBC and the female bias observed in the human disease.

Materials and Methods

GENERATION OF ARE-DEL$^{-/-}$ MICE

The generation of this strain has been described,[18] and the phenotype has been described as including a mild lupus-like disease. However, we observed that sera from older mice appeared fatty, and this led to the studies reported herein; two ARE-Del lines, derived from individual embryonic stem cell clones, were selected and backcrossed at least 10 generations onto C57BL/6 mice. After backcrossing, the genetic backgrounds were assessed at the DartMouse Speed Congenic Core Facility at the Geisel School of Medicine at Dartmouth. Animal care was provided in accordance with the procedures outlined in the "Guide for Care and Use of Laboratory Animals" (National Research Council, 2011).

HISTOPATHOLOGY

Detailed protocols of hematoxylin and eosin (H&E) staining, sirius red staining, Fontana-Masson staining, and histological scoring are described in the Supporting Information.

DETECTION OF SERUM ANTI-MITOCHONDRIAL ANTIBODIES

Serum anti-mitochondrial antibodies (AMA) were detected using our standard enzyme-linked immunosorbent assay against recombinant proteins of the pyruvate dehydrogenase complex E2 subunit (PDC-E2), branched chain 2-oxo-acid dehydrogenase E2 subunit (BCOADC-E2), and 2-oxo-glutararte dehydrogenase E2 subunit (OGDC-E2).[19]

TOTAL BILE ACID ANALYSIS

Total bile acids (TBA) were analyzed using freshly collected serum and the Total Bile Acid Enzymatic Cycling Assay Kit (Diazyme, Poway, CA), according to the manufacturer's protocols with modifications as described in the Supporting Information.

RNA SEQUENCING

Detailed protocols, including messenger RNA preparation, library construction, Illumina HiSeq2500 sequencing, and data processing, are described in the Supporting Information. The data set is available in the National Center for Biotechnology Information/Gene Expression Omnibus (GSE76309).

ADOPTIVE CELL TRANSFER

Spleen cells were collected from 20-week-old female ARE-Del$^{-/-}$ mice. Mononuclear cells were isolated, and CD4^{+} or CD8^{+} T cells were purified by positive selection with microbeads and MiniMacs separation columns. Ten-week-old female B6/Rag1$^{-/-}$ mice were used as recipients. CD4^{+} T cells, CD8^{+} T cells, or whole spleen mononuclear cells (1×10^{6}) were transferred into recipient mice by tail vein injection.

ARTICLE INFORMATION:

From the [1]Cancer and Inflammation Program, Center for Cancer Research, National Cancer Institute-Frederick, Frederick, MD; [2]Division of Rheumatology, Allergy and Clinical Immunology, University of California Davis School of Medicine, Davis, CA; [3]Department of Pathology and Laboratory Medicine, Institute of Biomedical Sciences, Tokushima University Graduate School, Japan; [4]Laboratory of Animal Science, National Cancer Institute-Frederick, Frederick, MD; [5]CCR Collaborative Bioinformatics Core, National Cancer Institute, Bethesda, MD; [6]Central Laboratory Kagawa Prefectural Central Hospital, Takamatsu, Japan; [7]Laboratory of Liver Diseases, National Institute on Alcohol Abuse and Alcoholism, Rockville, MD; [8]The Russell H. Morgan Department of Radiology and Radiological Science, Johns Hopkins University School of Medicine, Baltimore, MD.

ADDRESS CORRESPONDENCE AND REPRINT REQUESTS TO:

Howard Young, Ph.D.
Cancer and Inflammation Program, Center for Cancer Research
National Cancer Institute-Frederick
Frederick, MD 21702; or

M. Eric Gershwin, M.D.
Division of Rheumatology, Allergy and Clinical Immunology
University of California Davis School of Medicine
Davis, CA 95616

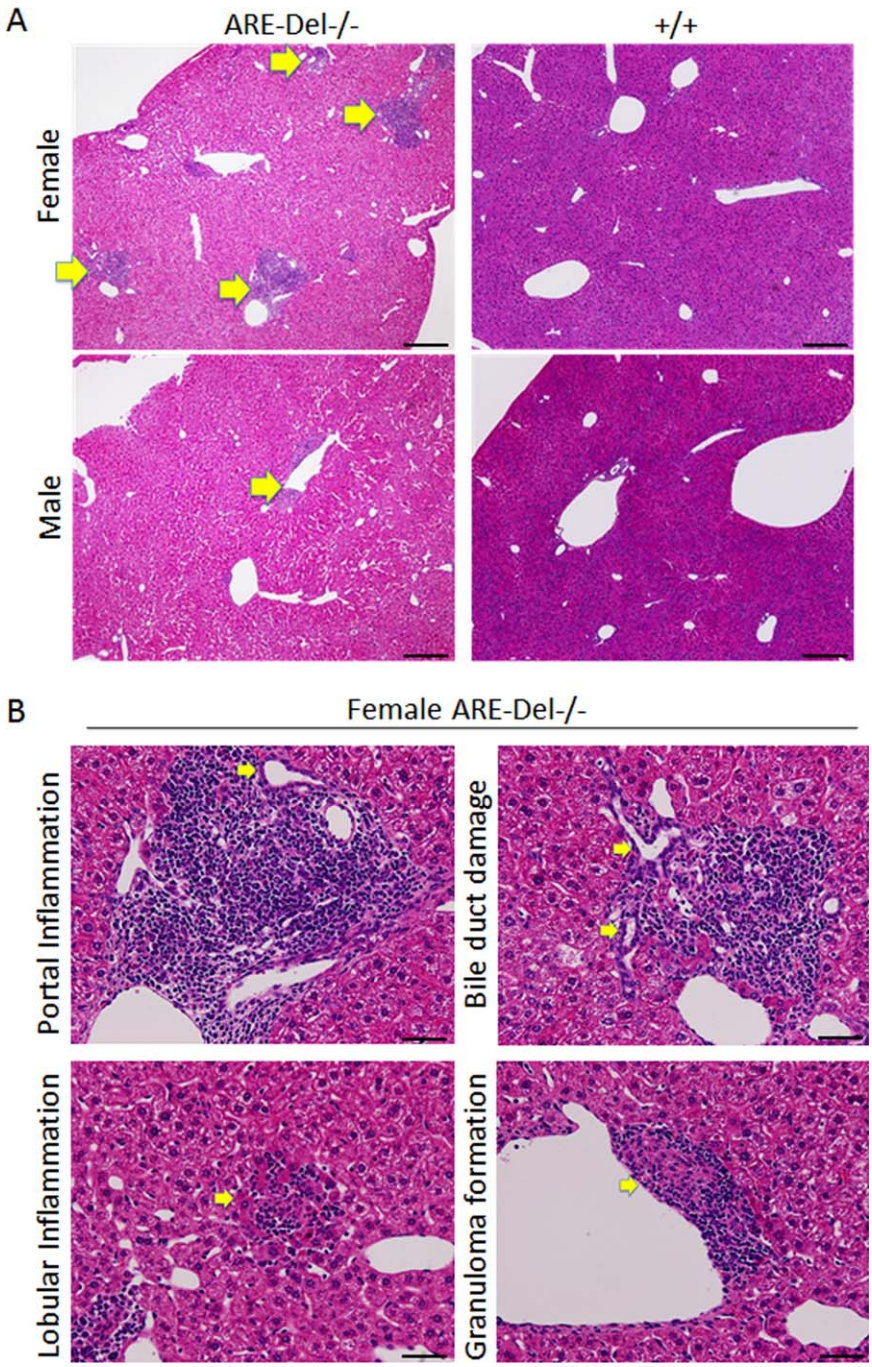

FIG. 1. Liver histology in ARE-Del$^{-/-}$ mice. (A) Representative H&E staining of male and female ARE-Del$^{-/-}$ mice. Arrows point to the inflammatory foci region. (B) Representative H&E staining of portal inflammation (arrow: bile duct showing mild damage), lobular inflammation (arrow: focal necrosis), biliary duct damage (arrow: bile duct showing moderate damage), and granuloma formation (arrow: epithelioid granuloma in portal tract) in female ARE-Del$^{-/-}$ mice. (C) Statistical analysis of liver histology of male and female ARE-Del$^{-/-}$ mice was performed by the nonparametric Mann-Whitney test using GraphPad Prism 6.0 (mean ± standard error of the mean, n = 16 from three independent experiments). The two-tailed P value <0.05 was taken as significant ($^{*}P < 0.05$, $^{**}P < 0.01$, $^{***}P < 0.001$). (D) Representative sirius red staining of liver fibrosis in female ARE-Del$^{-/-}$ mice at age 20 weeks. Scale bars = 200 μm (A), 50 μm (B) and 100 μm (D).

EVALUATION OF PATHOLOGICAL CHANGE IN RECIPIENT MICE

At 20 weeks after cell transfer, mice were sacrificed and livers were collected for H&E staining. The histopathology was graded as no inflammation (or bile duct damage), minimal inflammation (or bile duct damage), mild inflammation (or bile duct damage), moderate inflammation (or bile duct damage), and severe inflammation (or bile duct damage). Levels of IFN, tumor necrosis factor (TNF), interleukin-6 (IL-6), and monocyte chemoattractant protein-1 (MCP-1) in serum of recipient mice were measured with a cytokine

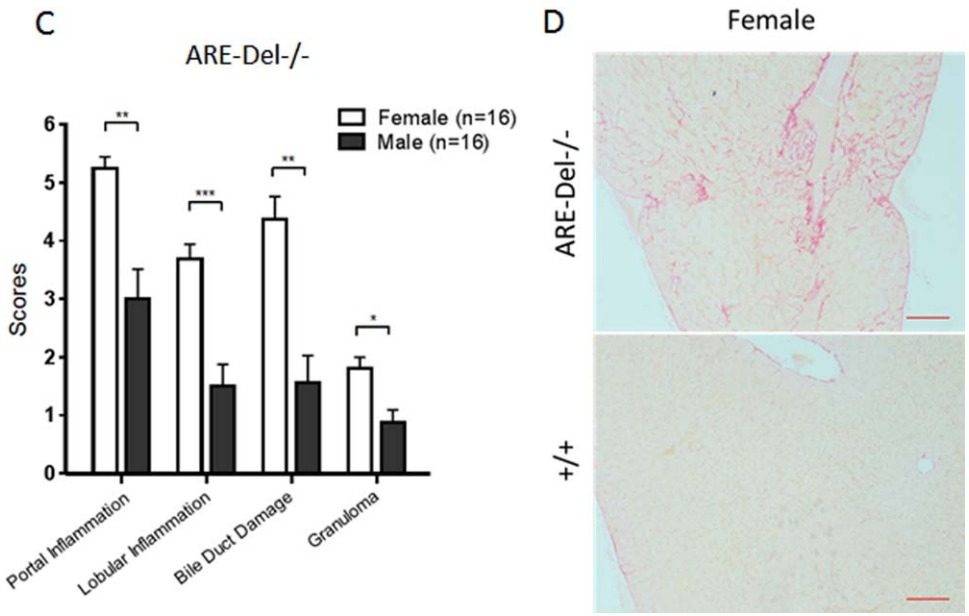

FIG. 1. Continued

bead array assay using the Mouse Inflammatory Cytokine Kit.

Results

PORTAL AND LOBULAR INFLAMMATION, BILE DUCT DAMAGE, FIBROSIS, AND GRANULOMA FORMATION IN ARE-DEL$^{-/-}$ MICE WITH FEMALE DOMINANCE

Hepatic lesions from 20-week-old female ARE-Del$^{-/-}$ mice were noted to have moderate to severe portal lymphoid cell infiltration, whereas male ARE-Del$^{-/-}$ had only mild to moderate infiltration (Fig. 1A). Furthermore, portal and lobular inflammation, small bile duct destruction, and granuloma formation were more severe in female ARE-Del$^{-/-}$ mice (Fig. 1B). We further assessed the severity of these hepatic lesions based on unbiased quantification of frequency (Fig. 1C). A Mann-Whitney statistical analysis of all ages of mice (8-10 weeks old n = 4, 19-24 weeks n = 8, over 40 weeks n = 4) demonstrated that female ARE-Del$^{-/-}$ mice had higher frequencies of lymphocyte infiltration, damaged bile ducts, and granulomas than male ARE-Del$^{-/-}$ mice. Bile duct destruction correlated with age, indicating that bile duct damage occurs at a later stage of progression (Supporting Fig. S1). Based on sirius red staining (Fig. 1D), mild fibrosis was observed in female ARE-Del$^{-/-}$ mice; the severity of fibrosis was substantially lower or not detectable in male ARE-Del$^{-/-}$ mice (data not shown).

Both aspartate aminotransferase and alanine aminotransferase levels were significantly increased in 20-week-old female ARE-Del$^{-/-}$ mice, although not as high as one finds in models of hepatitis.[20] Male ARE-Del$^{-/-}$ mice had significant changes in the level of alanine aminotransferase compared to control littermates, but there were no significant changes in the level of aspartate aminotransferase (Supporting Fig. S2). Considering that alanine aminotransferase is exclusively in the cytoplasm while aspartate aminotransferase is in both mitochondria and the cytoplasm, this result suggests that female ARE-Del$^{-/-}$ mice may have critical damage in the mitochondria of target cells.

FEMALE ARE-DEL$^{-/-}$ MICE PRODUCE AMA

Female ARE-Del$^{-/-}$ mice, 8-10 weeks old, had readily detectable antibodies to PDC-E2, BCOADC-E2, and OGDC-E2 (Fig. 2A). These data were replicated at 20 weeks of age (Fig. 2C). The dominant autoantibody was directed to PDC-E2. In contrast, male ARE-Del$^{-/-}$ mice, 8-10 weeks old, had detectable

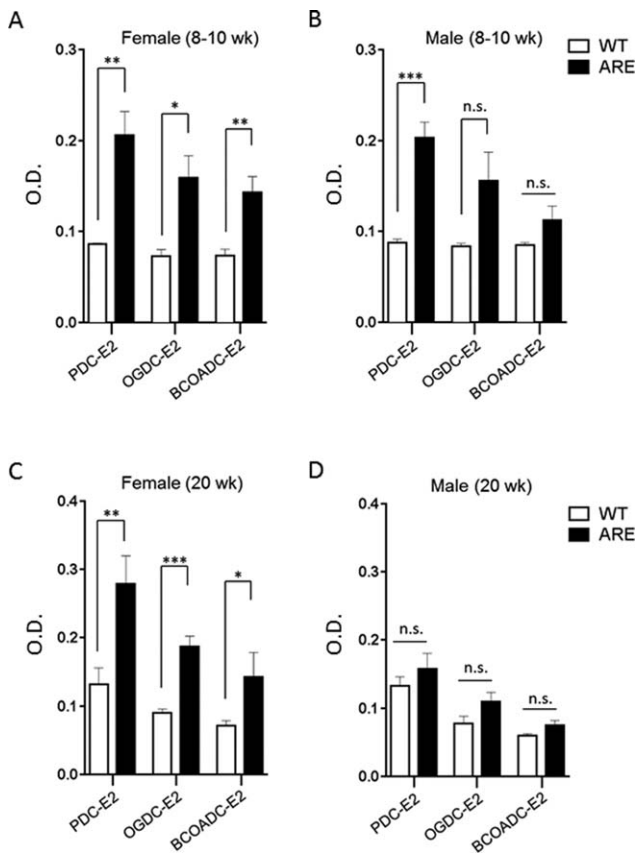

FIG. 2. Levels of AMA in ARE-Del$^{-/-}$ mice. (A,B) Level of anti-PDC-E2, anti-OGDC-E2, and anti-BCOADC-E2 in the serum of female (A) and male (B) ARE-Del$^{-/-}$ at age 10 (±2) weeks (n = 4). (C,D) Levels of anti-PDC-E2, anti-OGDC-E2, and anti-BCOADC-E2 in the serum of female (C) and male (D) ARE-Del$^{-/-}$ mice at age 20 (±2) weeks (n = 7-8). Data represent mean ± standard error of the mean. Statistical analysis was performed by unpaired Student *t* test. All data are representative of at least three independent experiments. $^{*}P < 0.05$; $^{**}P < 0.01$; $^{***}P < 0.001$. Abbreviations: n.s., not significant; O.D., optical density; WT, wild type.

antibodies to PDC-E2 but no significant differences from controls with respect to autoantibodies to OGDC-E2 or BCOADC-E2 (Fig. 2B). Interestingly, at 20 weeks of age, there were no significant detectable AMA to any of the three epitopes in the male groups compared to controls (Fig. 2D).

TBA ARE HIGHLY UP-REGULATED IN FEMALE ARE-DEL$^{-/-}$ MICE

Eight-week-old female ARE-Del$^{-/-}$ mice had a mild elevation of TBA (25.8 ± 3.67 μM, n = 4). There were no significant changes observed in male ARE-Del$^{-/-}$ mice (Fig. 3A). In contrast, significantly higher levels of TBA were observed in 20-week-old female ARE-Del$^{-/-}$ mice (115.6 ± 11.71 μM of mean ± standard error of the mean, n = 8) versus control littermates (3.8 ± 0.36 μM, n = 9). Male ARE-Del$^{-/-}$ mice had relatively mild induction of TBA (19.12 ± 5.5 μM, n = 8) compared to control littermates (1.9 ± 0.36 μM, n = 8) (Fig. 3B). Linear regression was performed to analyze the correlation coefficient of the serum TBA with histological scores of lymphocytic infiltration, bile duct damage, and granuloma formation. In 8-10 weeks, there was no correlation between TBA and the histological scores (Supporting Fig. S3A), whereas 20-week-old mice had relatively significant correlations of TBA with portal inflammation ($r = 0.79$), lobular inflammation ($r = 0.76$), bile duct damage ($r = 0.80$), and granuloma formation ($r = 0.91$) (Supporting Fig. S3B). Skin hyperpigmentation, a characteristic feature of PBC, was increased in 20-week-old female ARE-Del$^{-/-}$ mice (Fig. 3C), potentially through inadequate bile flow due to bile duct destruction. Male

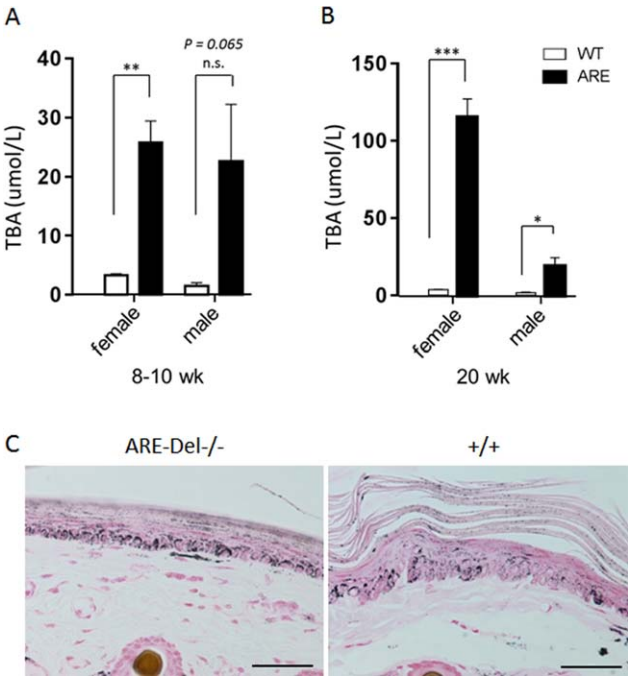

FIG. 3. Serum TBA levels in ARE-Del$^{-/-}$ mice. (A) Serum TBA levels in female and male ARE-Del$^{-/-}$ mice at age 10 (±2) weeks (n = 4). (B) Serum TBA levels in female and male ARE-Del$^{-/-}$ mice at age 20 (±2) weeks (n = 7-8). Data represent mean ± standard error of the mean. Statistical analysis was performed by unpaired Student *t* test. $^{*}P < 0.05$, $^{**}P < 0.01$, $^{***}P < 0.001$. (C) Increased tail skin pigmentation in female ARE-Del$^{-/-}$ mice. Scale bars = 100 μm. All data are representative of at least three independent experiments. Abbreviations: n.s., not significant; WT, wild type.

ARE-Del$^{-/-}$ mice had mild or no increased skin hyperpigmentation, similar to that observed in ARE-Del$^{+/-}$ heterozygotes. Overall, the level of TBA was correlated with the level of skin pigmentation in both ARE-Del$^{-/-}$ and ARE-Del$^{+/-}$ mice (data now shown).

FEMALE-SPECIFIC DISEASE PROGRESSION IS CHARACTERISTIC OF ARE-DEL HETEROZYGOTES

ARE-Del heterozygote mice have approximately 50% the level of circulating IFN compared to homozygous mice. We evaluated liver histology in heterozygous mice compared to female ARE-Del$^{-/-}$ mice (Fig. 4A). Although the overall image-based severity of hepatic lesions of female ARE-Del$^{+/-}$ was less than that of female ARE-Del$^{-/-}$ mice, the histological scores of inflammatory regions indicated that female ARE-Del$^{+/-}$ mice had portal tract lymphocytic infiltrates and biliary duct lesions similar to female ARE-Del$^{-/-}$ mice. In contrast, male ARE-Del$^{+/-}$ mice had much lower severity in lesions, consistent with the hypothesis that female mice are more sensitive and/or amplify the IFN signaling pathway compared to male mice (Fig. 4B,C). We further analyzed serum AMA (Fig. 4D,E) and TBA (Fig. 4F) of ARE-Del$^{+/-}$ mice. In 20-week-old mice, the level of AMA was significantly up-regulated in female, but not male, ARE-Del$^{+/-}$ mice, similar to that observed in ARE-Del$^{-/-}$ mice. Serum levels of TBA were mildly increased in female ARE-Del$^{+/-}$ mice and did not correlate with histologic scores, unlike the above data on female ARE-Del$^{-/-}$ mice (Supporting Fig. S3C).

GENE EXPRESSION SIGNATURES IN ARE-DEL$^{-/-}$ MICE

A Venn diagram presentation of the data reflects that female ARE-Del$^{-/-}$ mice have 1118 differentially expressed genes compared to control littermates and that male ARE-Del$^{-/-}$ mice have 288 differentially expressed genes based on the criteria of greater than ±2-fold changes and a false discovery rate <0.05 (Fig. 5A). There are 258 genes commonly overexpressed by female and male ARE-Del$^{-/-}$ mice, demonstrating that the majority of genes from male ARE-Del$^{-/-}$ mice are differentially expressed compared to female ARE-Del$^{-/-}$ mice. A heat map generated from these overlapping genes demonstrates that female ARE-Del$^{-/-}$ mice have stronger expression of these genes (Fig. 5B). Considering that male ARE-Del$^{-/-}$ mice have only mild to moderate pathology, these overlapping gene expression patterns of both female and male ARE-Del$^{-/-}$ mice suggest their involvement in the initiation of autoimmune cholangitis. To explore the possible mechanism, we performed a pathway analysis of these 258 genes using Ingenuity Pathway Analysis (IPA). In this analysis, IFNγ (P value as 4.5×10^{-38}) and the IFNα receptor (P value as 4.5×10^{-26}) were observed as top upstream regulators, while IFN signaling was more predominant in female ARE-Del$^{-/-}$ mice (Fig. 5C). Consistent with gene expression data, we further confirmed higher levels of serum IFNγ in female versus male ARE-Del$^{-/-}$ mice (Supporting Fig. S4). There was also significant stronger induction of chemokines (monokine induced by IFNγ, IFNγ-inducible protein 10, and macrophage inflammatory protein 1beta) and cytokines (TNFα, IL-10, and IL-13) in female ARE-Del$^{-/-}$, whereas other cytokines and chemokines were not significantly altered. The antigen presentation pathway was detectable as a top canonical pathway for the 258 overlapping genes (Fig. 5D), and major histocompatibility complex II (MHC-II) genes were the most highly expressed genes in both male and female ARE-Del$^{-/-}$ mice (Table 1), indicating that this pathway is likely critical for the initiation of this disease.

SIMILARITY OF GENE SIGNATURES BETWEEN HUMAN AND ARE-DEL$^{-/-}$ MICE

Gene expression analysis on liver biopsy tissues from PBC patients indicated that IFNγ signaling was significantly detectable in both early and late stages of disease.[21-23] Most of all, up-regulation of IFNγ signaling was more evident on chronic nonsuppurative destructive cholangitis and biliary epithelial cell (BEC) lesions dissected by laser capture microdissection. As BECs are the target cells in PBC, we compared the gene expression profile of this lesion with ARE-Del$^{-/-}$ mice. Using the full list of genes in PBC-BEC lesions biopsied from PBC patients ($n = 5$) versus normal subjects ($n = 3$), we analyzed 78 differentially induced genes and performed gene set enrichment analysis of these genes in the human subject data using gene sets from ARE-Del$^{-/-}$ mice. Notably, IFNγ was detectable as a top upstream regulator (P value as 4.2×10^{-29}), and there was a significant enrichment of the human gene data in the data obtained from both male and female ARE-Del$^{-/-}$ mice (Fig. 6A,B), suggesting that IFNγ may play a pathogenic role in BECs in the early stage of PBC disease. Based on the similar expression pattern of representative human genes (Supporting Table S1), H2-Aa (human leukocyte antigen DQA1)

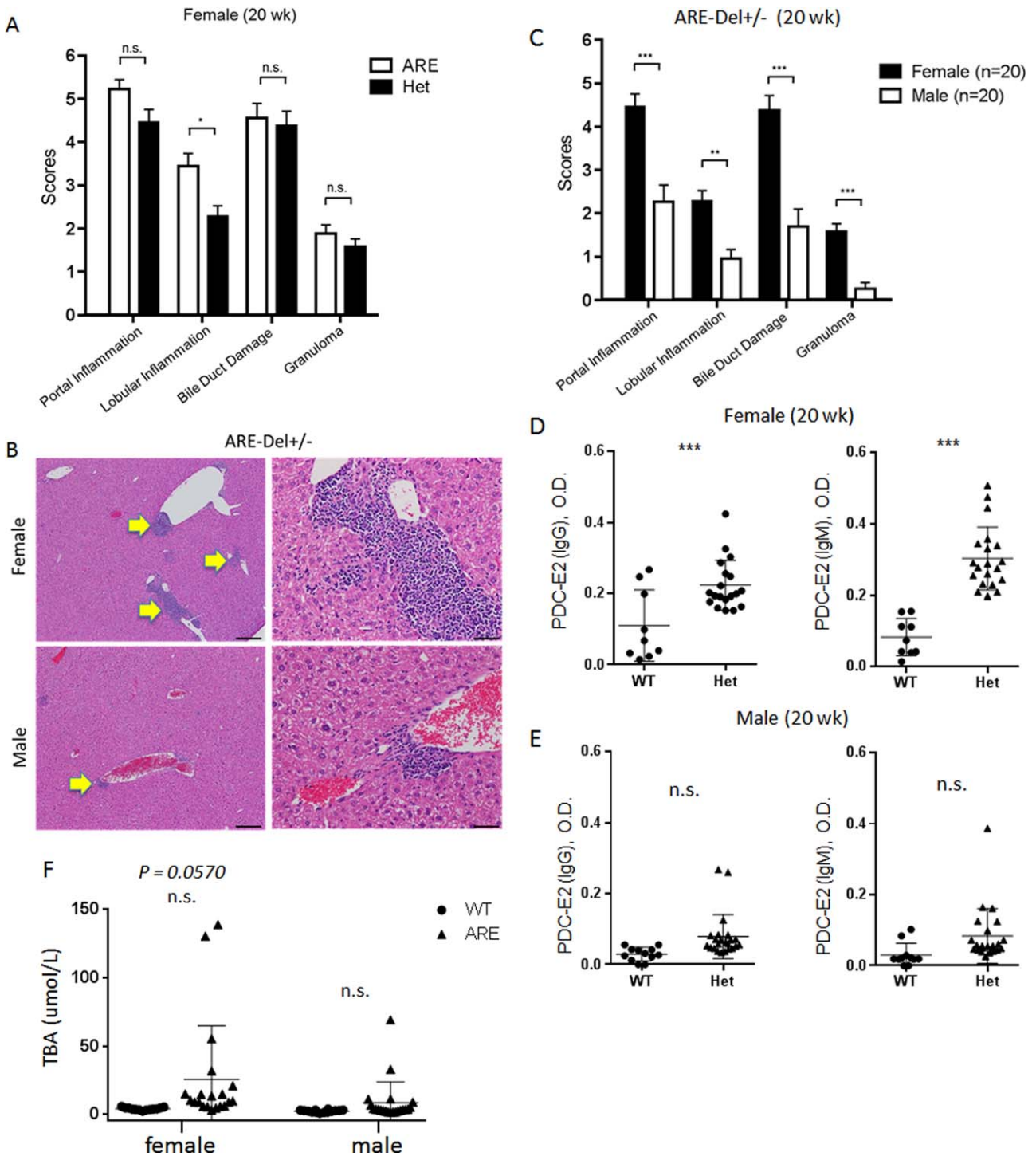

FIG. 4. Pathology of ARE-Del heterozygotes versus homozygotes. (A) Statistical analysis of female ARE-Del$^{-/-}$ mice (n = 9 from two independent experiments) versus ARE-Del$^{+/-}$ mice (n = 23 from two independent experiments) with portal inflammation, lobular inflammation, biliary damage, and granuloma formation at age 20 weeks (mean ± standard error of the mean), performed by nonparametric Mann-Whitney test with a two-tailed *p*-value. (B) Representative H&E staining of male and female ARE-Del$^{+/-}$ mice at age 20 weeks. Arrows point to the inflammatory foci region. Scale bars = 200 μm (B left) and 50 μm (B right) (C) Statistical analysis of liver histology of male and female ARE-Del$^{+/-}$ mice (n = 20 ± 2 from two independent experiments) was performed by Mann-Whitney test with a two-tailed *p*-value. (D,E) Immunoglobulins G and M anti-PDC-E2 in male and female ARE-Del$^{+/-}$ mice at age 20 weeks (mean ± standard deviation, n = 20 ± 2). (F) Serum TBA in male and female ARE-Del$^{+/-}$ mice at age 20 weeks (mean ± standard deviation, n = 20 ± 2). (D-F) Statistical analysis was performed by unpaired Student *t* test.*$P < 0.05$, **$P < 0.01$, ***$P < 0.001$. Abbreviations: Het, heterozygote; IgG/IgM, immunoglobulins G and M; n.s., not significant; O.D., optical density; WT, wild type.

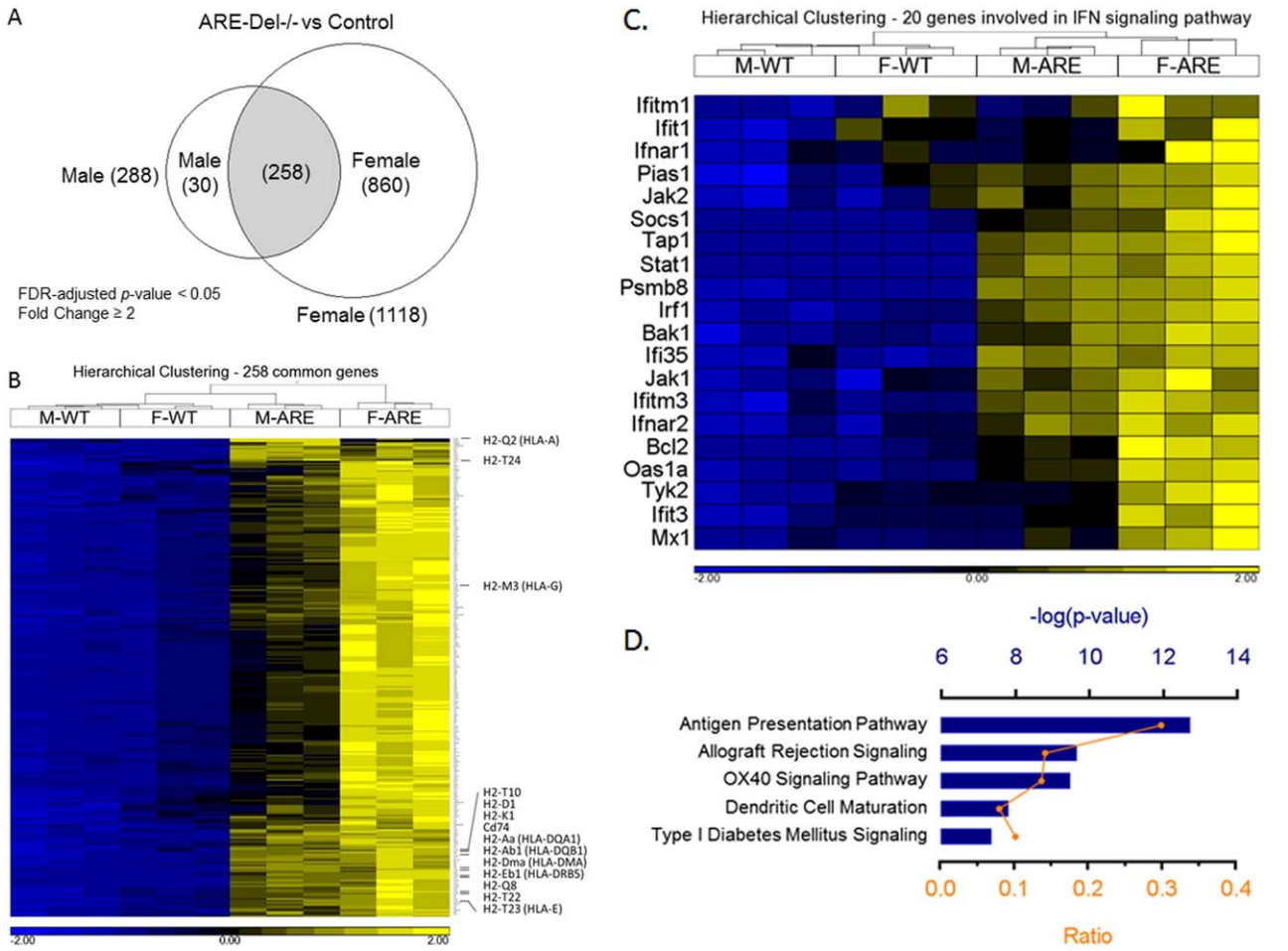

FIG. 5. Hepatic gene expression in male and female ARE-Del$^{-/-}$ mice at age 20 weeks. (A) Venn diagram of differentially expressed genes in male and female ARE-Del$^{-/-}$ mice versus control mice (n = 3). (B) Hierarchical clustering of 258 common genes. The human homologs are described in parentheses. (C) Hierarchical clustering of 20 genes involved in the IFN signaling pathway. (D) Top canonical pathways of common genes derived from IPA. Ratio (bottom *y* axis, yellow line) refers to the number of genes from the data set divided by the total number of genes that make up that pathway from within the IPA knowledge base, and the -log of the *P* value (top *y* axis, bar) was calculated by Fisher's exact test. Abbreviations: F, female; FDR, false discovery rate; HLA, human leukocyte antigen; M, male; WT, wild type.

expression was one of most significantly induced genes in ARE-Del$^{-/-}$ mice. It has been reported that the protein expression of human leukocyte antigen DQA1 was highly increased in BEC lesions from PBC patients[24] and that the MHC II locus was significantly associated with susceptibility to PBC[25,26]; thus, our data consistently imply the importance of MHC class II expression in BECs for the initiation stage of PBC.

We performed IPA of 253 genes from Italian patient cohorts selected by a pathway-based linear combination test.[27] Remarkably, we identified IFNγ as the top upstream regulator (*P* value as 1.8×10^{-15}) in these genes (Supporting Fig. S5). Furthermore, based on recent genome-wide association studies (GWASs),[24,28-30] we performed pathway analysis of 26 genes (Supporting Table S2) that have the most significant variants (*P* value $\leq 1 \times 10^{-5}$), selected by the National Human Genome Research Institute GWAS Catalog.[31] Twenty-one among the 26 genes were connected to IFNγ-mediated signaling, and IFNγ was also consistently detectable as the top upstream regulator (*P* value as 8.7×10^{-9}) as core networks were generated (Fig. 6C). Among the top canonical pathways of these genes, Th-cell differentiation, dendritic cell maturation, and B-cell development were identified as highly significant; and these pathways strongly overlapped with those identified in female ARE-Del$^{-/-}$ mice (Fig. 6D). Target DE genes from female ARE-Del$^{-/-}$ mice for each

TABLE 1. Up-regulation of MHC Class I and II Genes in ARE-Del$^{-/-}$ Mice

		ARE-Del$^{-/-}$ (Male)		ARE-Del$^{-/-}$ (Female)	
MHC	Gene	*P*	Fold	*P*	Fold
Class II	Cd74	1.54×10^{-5}	44.5	6.26×10^{-6}	37.4
	H2-DMa	3.64×10^{-4}	40.6	5.55×10^{-5}	33.7
	H2-Aa	2.96×10^{-4}	34.1	7.95×10^{-5}	30.0
	H2-Eb1	1.97×10^{-4}	27.0	1.69×10^{-5}	30.0
	H2-Ab1	1.26×10^{-4}	21.1	1.48×10^{-5}	22.5
Class I	H2-Q2	1.57×10^{-6}	23.7	3.0×10^{-3}	4.4
	H2-Q8	2.95×10^{-4}	4.8	4.65×10^{-5}	3.9
	H2-M3	9.19×10^{-6}	4.1	1.48×10^{-7}	4.3
	H2-T10	1.69×10^{-5}	3.9	2.34×10^{-5}	2.6
	H2-T23	8.59×10^{-6}	3.8	1.59×10^{-6}	3.2
	H2-D1	7.44×10^{-8}	3.2	1.88×10^{-8}	3.1
	H2-K1	4.89×10^{-7}	3.0	4.80×10^{-7}	2.5
	H2-T24	9.70×10^{-4}	2.8	2.41×10^{-4}	2.0
	H2-T22	2.90×10^{-5}	2.7	6.23×10^{-6}	2.4

pathway are listed (Supporting Table S3), and their gene networks also indicated Ifng, Ifnar, Tnf, Il-10, and Il-1b as top upstream regulator genes. Moreover, Th cell-mediated responses were specifically up-regulated in these pathways, and immunohistochemical staining with anti-CD4 and anti-CD8 antibodies consistently showed higher CD4 infiltration in chronic nonsuppurative destructive cholangitis lesions of female ARE-Del$^{-/-}$ mice (Supporting Fig. S6). Thus, based on gene expression pathway analysis, the mouse model presented here and the human disease strongly overlap.

CD4 T CELLS ARE CRITICAL IN THE INDUCTION OF CHOLANGITIS IN ARE-DEL$^{-/-}$ MICE

Transfer of CD4 T cells from ARE-Del$^{-/-}$ mice to B6/Rag1$^{-/-}$ mice induced moderate portal inflammation and mild parenchymal inflammation, while bile duct damage and granuloma formation were minimally induced (Fig. 7A). As the transfer of CD4 T cells produced similar histological phenotypes with that observed upon transfer of whole spleen cells, CD4 T cells may thus have a critical role in the pathological progression observed in ARE-Del$^{-/-}$ mice. In contrast, transfer of CD8 T cells resulted in minimal portal and parenchymal inflammation with no visible effects on bile ducts and no granuloma formation. The level of serum IFN, TNF-α, IL-6, and MCP-1 were consistently increased in mice receiving CD4 T cells or whole spleen cells (Fig. 7B). In comparison mice receiving CD8 T cells did not have significant induction of IFN, TNF-α and IL-6 compared with Rag1$^{-/-}$ mice; and only MCP-1 was enhanced similar to what was observed in mice receiving CD4 T cells.

Discussion

The data reported herein demonstrate that chronic expression of IFNγ leads to a classic PBC-like disease with female gender dominance. A number of murine spontaneous and induced models have been reported that manifest features of human PBC.[25,26,32-38] Clearly, no single model has fully mimicked the immunopathophysiology of human PBC, and none hitherto has exhibited female dominance. Immunologically, PBC has long been recognized as reflective of Th1-mediated autoimmunity. Our data indicate that the Th17 pathway suppresses the accumulation of IFNγ-producing cells in liver during the early phase of cholangitis, also supporting the hypothesis that IFNγ has a pivotal role in the early events in autoimmune cholangitis.[39] The expression of MHC in the liver is a major canonical pathway seen in both male and female ARE-Del$^{-/-}$ mice, indicating that IFNγ is critical for early stages of disease progression by enhancing MHC class expression.

Similar to a wide spectrum of autoimmune diseases, there is no convincing explanation or physiological mechanisms that accounts for the strong female predominance in PBC.[40] Epidemiological studies in PBC have suggested that frequent exposure to environmental chemicals such as nail polish, chemicals found in tobacco smoke, and use of hormone replacement therapies are significantly associated with an increased risk of PBC.[41] Other risk factors implicated in female predominance of PBC include recurrent urinary tract infection in females, use of exogenous estrogens, as well as an increased prevalence of reproductive complications.[42,43] These risk factors may work synergistically in accelerating loss of tolerance. Thus, we emphasize that it is not a genetic predisposition but rather the pathology mediated through the interplay of interferons as described above that results in disease pathology. For example, one may postulate that during infection or a chemical xenobiotic exposure there is a transient and local up-regulation of IFN, which in the genetically susceptible host will lead to loss of tolerance. Our data imply that these events may occur individually over time, each leading to an up-regulation of MHC on target tissue.

We focused on the female-specific pathways in ARE-Del$^{-/-}$ mice to investigate the mechanisms

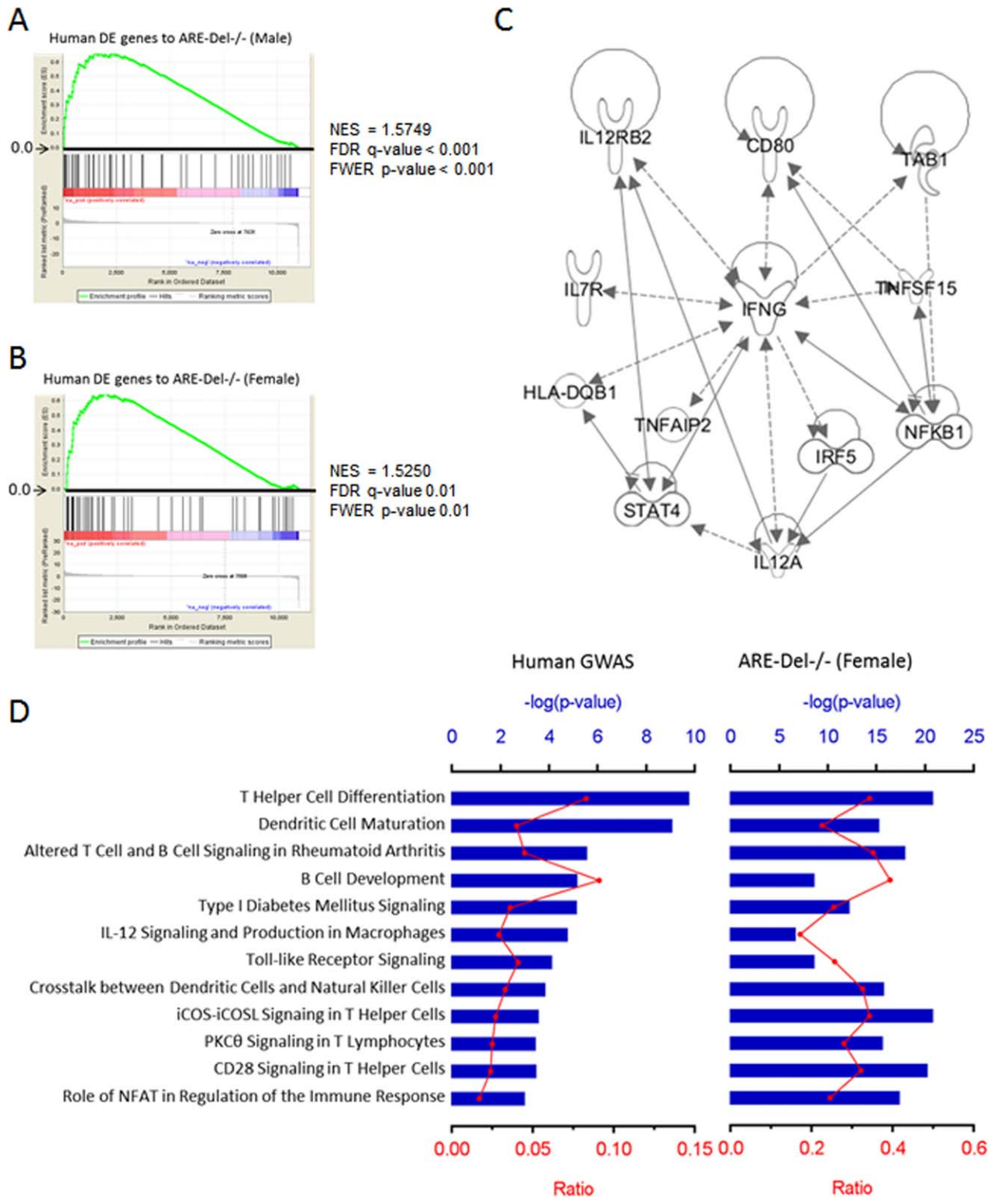

FIG. 6. Comparison of the gene expression profiling to human data from PBC patients. (A,B) Gene set enrichment analysis plots for human DE genes in PBC-BEC lesions using gene sets of male (A) and female (B) ARE-Del$^{-/-}$ mice. (C) Top network identified by IPA for the most significant 26 variants. The lines between genes represent known interactions (solid line for direct interaction, dashed line for indirect interaction). (D) Canonical pathways of human GWAS with ARE-Del$^{-/-}$ mice. The most significant 26 variants were selected by the National Human Genome Research Institute GWAS catalog ($p \leq 1 \times 10^{-5}$). Top canonical pathways of these genes were derived from IPA and compared with those from female ARE-Del$^{-/-}$ mice. "Ratio" (bottom *y* axis, yellow line) refers to the number of genes from the data set divided by the total number of genes that make up that pathway from within the IPA knowledge base, and the -log of the *P* value (top *y* axis, bar) was calculated by Fisher's exact test. Abbreviations: FDR, false discovery rate; FWER, family-wise error rate; iCOS/iCOSL, inducible costimulator/inducible costimulator ligand; NES, normalized enrichment scores; NFAT, nuclear factor of activated T cells; PKC, protein kinase C.

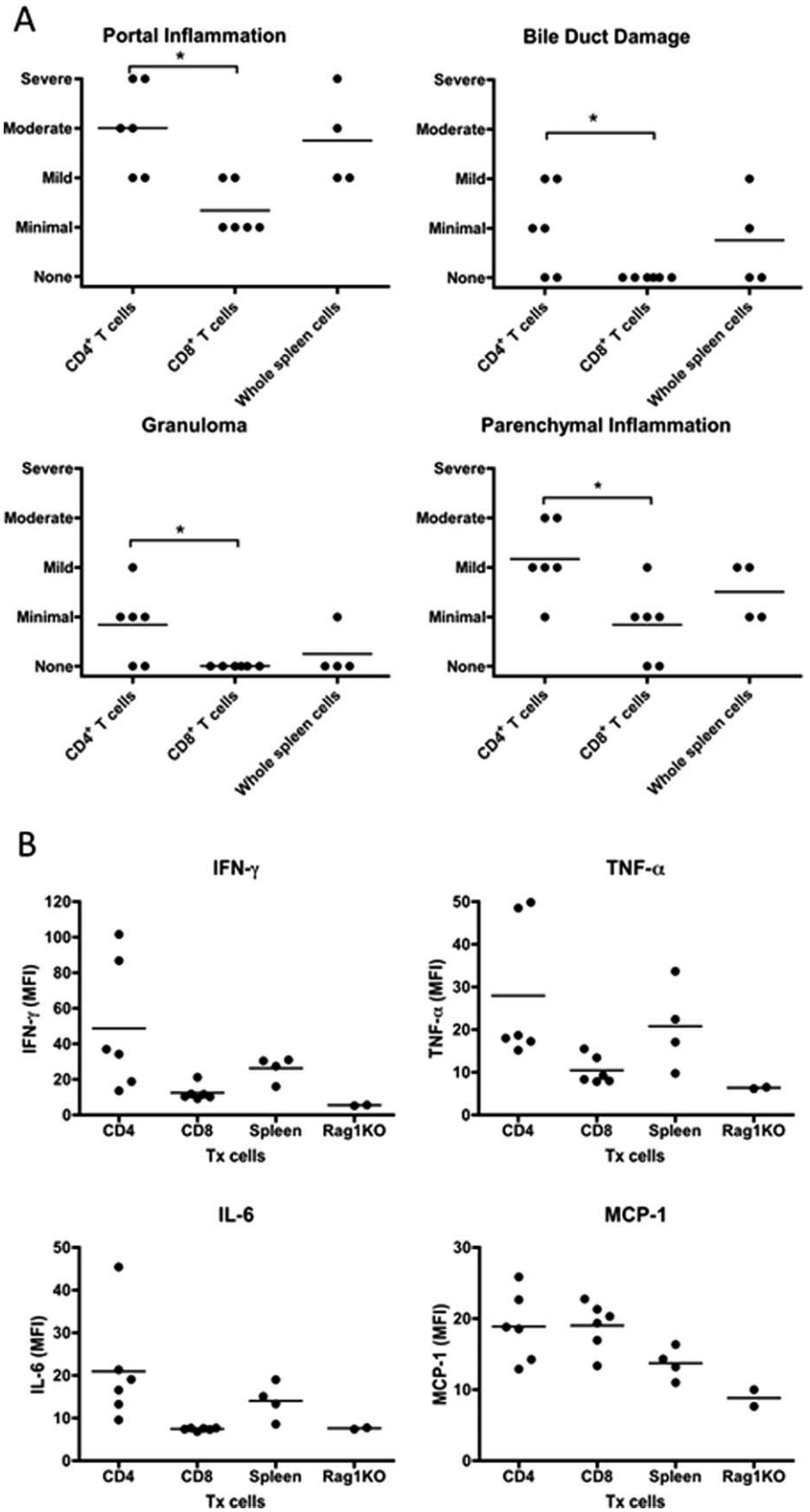

FIG. 7. Liver histopathology and level of inflammatory cytokines in recipient mice. (A) Pathological score of portal inflammation, bile duct damage, granuloma, and parenchymal inflammation in mice receiving $CD4^+$ T cells (n = 6), $CD8^+$ T cells (n = 6), and whole spleen cells (n = 4). (B) Serum were collected 20 weeks after cell transfer; the levels of IFN, TNF-α, IL-6, and MCP-1 in mice receiving $CD4^+$ T cells (n = 6), $CD8^+$ T cells (n = 6), and whole spleen cells (n = 4) were measured by a mouse inflammatory cytokine cytometric bead array kit. $^*P < 0.05$, $^{**}P < 0.01$, determined using the Kruskal-Wallis test (nonparametric analysis of variance). All data are representative of at least two independent experiments. Abbreviations: KO, knockout; MFI, mean fluorescence intensity.

involved in disease progression. Gene expression analysis showed that the immune response was critically affected in female ARE-Del$^{-/-}$ mice, especially in macrophages, dendritic cells, natural killer cells, and T and B cells. Importantly, Th cell-mediated signaling is one of the highly up-regulated pathways in female, but not in male, ARE-Del$^{-/-}$ mice. Interestingly, recent GWAS studies also point out that potential PBC causing single-nucleotide variants was enriched in CD4 T-cell signaling.[4] Of note, IL12-Janus kinase-signal transducer and activator of transcription 4 signaling in IL12-stimulated T cells may drive gender-biased susceptibility to autoimmune diseases due to enhanced Th1 responses as it has been reported that estrogen causes increased phosphorylation of signal transducer and activator of transcription 4 in a nonobese diabetic mouse model.[44] Consistent with our findings, CD4 T cells infiltrated in hepatic inflammatory lesions based on analysis of PBC liver biopsies,[4] and our cell transfer results also supported the model that CD4 T cells are critical for pathological progression of PBC. Therefore, our data suggest that IFNγ-induced Th1 response through CD4 T-cell activation drives the gender-biased progression of PBC.

In summary, this work presents evidence for a pathogenic role of IFNγ in the early stages and in the progression of PBC. Considering the prominence of a female-specific bias in PBC disease progression, further studies are necessary to investigate the mechanism of sex-biased interferon signaling and its effect on lymphocyte-mediated immune responses and on the mechanisms involved in IFNγ-mediated BEC death. Such studies will lead to a rational approach toward intervention and treatment of this chronic inflammatory disease.

Acknowledgment: We are grateful to Ian Mackay for his review and comments on the manuscript. We thank Ryosuke Bessho and Hayato Baba for help with image analysis, and Jinjung Choi, Charlotte Hanson, and Michael Sanford for help with technical assistance.

REFERENCES

1) Floreani A, Franceschet I, Perini L, Cazzagon N, Gershwin ME, Bowlus CL. New therapies for primary biliary cirrhosis. Clin Rev Allergy Immunol 2015;48:263-272.
2) Gershwin ME, Mackay IR, Sturgess A, Coppel RL. Identification and specificity of a cDNA encoding the 70 kd mitochondrial antigen recognized in primary biliary cirrhosis. J Immunol 1987;138:3525-3531.
3) Kaplan MM, Gershwin ME. Primary biliary cirrhosis. N Engl J Med 2005;353:1261-1273.
4) Webb GJ, Siminovitch KA, Hirschfield GM. The immunogenetics of primary biliary cirrhosis: a comprehensive review. J Autoimmun 2015;64:42-52.
5) Beuers U, Gershwin ME, Gish RG, Invernizzi P, Jones DE, Lindor K, et al. Changing nomenclature for PBC: from "cirrhosis" to "cholangitis." Dig Liver Dis 2015;39:e57-e59.
6) Dhirapong A, Yang GX, Nadler S, Zhang W, Tsuneyama K, Leung P, et al. Therapeutic effect of cytotoxic T lymphocyte antigen 4/immunoglobulin on a murine model of primary biliary cirrhosis. Hepatology 2013;57:708-715.
7) Huang W, Kachapati K, Adams D, Wu Y, Leung PS, Yang GX, et al. Murine autoimmune cholangitis requires two hits: cytotoxic KLRG1$^+$ CD8 effector cells and defective T regulatory cells. J Autoimmun 2014;50:123-134.
8) Li Y, Wang W, Tang L, He X, Yan X, Zhang X, et al. Chemokine (C-X-C motif) ligand 13 promotes intrahepatic chemokine (C-X-C motif) receptor 5+ lymphocyte homing and aberrant B-cell immune responses in primary biliary cirrhosis. Hepatology 2015;61:1998-2007.
9) Tomiyama T, Yang GX, Zhao M, Zhang W, Tanaka H, Wang J, et al. The modulation of co-stimulatory molecules by circulating exosomes in primary biliary cirrhosis. Cell Mol Immunol 2015; doi: 10.1038/cmi.2015.86.
10) Tsuda M, Ambrosini YM, Zhang W, Yang GX, Ando Y, Rong G, et al. Fine phenotypic and functional characterization of effector cluster of differentiation 8 positive T cells in human patients with primary biliary cirrhosis. Hepatology 2011;54:1293-1302.
11) Wang L, Sun Y, Zhang Z, Jia Y, Zou Z, Ding J, et al. CXCR5$^+$ CD4$^+$ T follicular helper cells participate in the pathogenesis of primary biliary cirrhosis. Hepatology 2015;61:627-638.
12) Chang CH, Chen YC, Yu YH, Tao MH, Leung PS, Ansari AA, et al. Innate immunity drives xenobiotic-induced murine autoimmune cholangitis. Clin Exp Immunol 2014;177:373-380.
13) Chang CH, Chen YC, Zhang W, Leung PS, Gershwin ME, Chuang YH. Innate immunity drives the initiation of a murine model of primary biliary cirrhosis. PloS One 2015;10:e0121320.
14) **Chuang YH**, **Lian ZX**, Tsuneyama K, Chiang BL, Ansari AA, Coppel RL, et al. Increased killing activity and decreased cytokine production in NK cells in patients with primary biliary cirrhosis. J Autoimmun 2006;26:232-240.
15) **Chuang YH**, **Lian ZX**, Yang GX, Shu SA, Moritoki Y, Ridgway WM, et al. Natural killer T cells exacerbate liver injury in a transforming growth factor beta receptor II dominant-negative mouse model of primary biliary cirrhosis. Hepatology 2008;47:571-580.
16) Kawata K, Kobayashi Y, Gershwin ME, Bowlus CL. The immunophysiology and apoptosis of biliary epithelial cells: primary biliary cirrhosis and primary sclerosing cholangitis. Clin Rev Allergy Immunol 2012;43:230-241.
17) Lleo A, Bowlus CL, Yang GX, Invernizzi P, Podda M, Van de Water J, et al. Biliary apotopes and anti-mitochondrial antibodies activate innate immune responses in primary biliary cirrhosis. Hepatology 2010;52:987-998.
18) Hodge DL, Berthet C, Coppola V, Kastenmuller W, Buschman MD, Schaughency PM, et al. IFN-gamma AU-rich element

removal promotes chronic IFN-gamma expression and autoimmunity in mice. J Autoimmun 2014;53:33-45.
19) Moteki S, Leung PS, Coppel RL, Dickson ER, Kaplan MM, Munoz S, et al. Use of a designer triple expression hybrid clone for three different lipoyl domain for the detection of antimitochondrial autoantibodies. HEPATOLOGY 1996;24:97-103.
20) Lafdil F, Wang H, Park O, Zhang W, Moritoki Y, Yin S, et al. Myeloid STAT3 inhibits T cell-mediated hepatitis by regulating T helper 1 cytokine and interleukin-17 production. Gastroenterology 2009;137:2125-2135.
21) Baba N, Kobashi H, Yamamoto K, Terada R, Suzuki T, Hakoda T, et al. Gene expression profiling in biliary epithelial cells of primary biliary cirrhosis using laser capture microdissection and cDNA microarray. Transl Res 2006;148:103-113.
22) Honda M, Kawai H, Shirota Y, Yamashita T, Kaneko S. Differential gene expression profiles in stage I primary biliary cirrhosis. Am J Gastroenterol 2005;100:2019-2030.
23) Shackel NA, McGuinness PH, Abbott CA, Gorrell MD, McCaughan GW. Identification of novel molecules and pathogenic pathways in primary biliary cirrhosis: cDNA array analysis of intrahepatic differential gene expression. Gut 2001;49:565-576.
24) **Mells GF**, **Floyd JA**, **Morley KI,** Cordell HJ, Franklin CS, Shin SY, et al. Genome-wide association study identifies 12 new susceptibility loci for primary biliary cirrhosis. Nat Genet 2011; 43:329-332.
25) Katsumi T, Tomita K, Leung PS, Yang GX, Gershwin ME, Ueno Y. Animal models of primary biliary cirrhosis. Clin Rev Allergy Immunol 2015;48:142-153.
26) Wakabayashi K, Lian ZX, Leung PS, Moritoki Y, Tsuneyama K, Kurth MJ, et al. Loss of tolerance in C57BL/6 mice to the autoantigen E2 subunit of pyruvate dehydrogenase by a xenobiotic with ensuing biliary ductular disease. HEPATOLOGY 2008;48:531-540.
27) Kar SP, Seldin MF, Chen W, Lu E, Hirschfield GM, Invernizzi P, et al. Pathway-based analysis of primary biliary cirrhosis genome-wide association studies. Genes Immun 2013;14:179-186.
28) Hirschfield GM, Liu X, Xu C, Lu Y, Xie G, Gu X, et al. Primary biliary cirrhosis associated with HLA, IL12A, and IL12RB2 variants. N Engl J Med 2009;360:2544-2555.
29) **Liu X**, **Invernizzi P**, Lu Y, Kosoy R, Bianchi I, Podda M, et al. Genome-wide meta-analyses identify three loci associated with primary biliary cirrhosis. Nat Genet 2010;42:658-660.
30) **Nakamura M**, **Nishida N**, Kawashima M, Aiba Y, Tanaka A, Yasunami M, et al. Genome-wide association study identifies TNFSF15 and POU2AF1 as susceptibility loci for primary biliary cirrhosis in the Japanese population. Am J Hum Genet 2012; 91:721-728.
31) Welter D, MacArthur J, Morales J, Burdett T, Hall P, Junkins H, et al. The NHGRI GWAS Catalog, a curated resource of SNP-trait associations. Nucleic Acids Res 2014;42:D1001-D1006.
32) Irie J, Wu Y, Wicker LS, Rainbow D, Nalesnik MA, Hirsch R, et al. NOD.c3c4 congenic mice develop autoimmune biliary disease that serologically and pathogenetically models human primary biliary cirrhosis. J Exp Med 2006;203:1209-1219.
33) Oertelt S, Lian ZX, Cheng CM, Chuang YH, Padgett KA, He XS, et al. Anti-mitochondrial antibodies and primary biliary cirrhosis in TGF-beta receptor II dominant-negative mice. J Immunol 2006;177:1655-1660.
34) Salas JT, Banales JM, Sarvide S, Recalde S, Ferrer A, Uriarte I, et al. Ae2a,b-deficient mice develop antimitochondrial antibodies and other features resembling primary biliary cirrhosis. Gastroenterology 2008;134:1482-1493.
35) Wakabayashi K, Lian ZX, Moritoki Y, Lan RY, Tsuneyama K, Chuang YH, et al. IL-2 receptor alpha$^{-/-}$ mice and the development of primary biliary cirrhosis. HEPATOLOGY 2006;44:1240-1249.
36) Wang J, Yang GX, Tsuneyama K, Gershwin ME, Ridgway WM, Leung PS. Animal models of primary biliary cirrhosis. Semin Liver Dis 2014;34:285-296.
37) Wang JJ, Yang GX, Zhang WC, Lu L, Tsuneyama K, Kronenberg M, et al. *Escherichia coli* infection induces autoimmune cholangitis and anti-mitochondrial antibodies in non-obese diabetic (NOD).B6 (Idd10/Idd18) mice. Clin Exp Immunol 2014;175:192-201.
38) Zhang W, Sharma R, Ju ST, He XS, Tao Y, Tsuneyama K, et al. Deficiency in regulatory T cells results in development of antimitochondrial antibodies and autoimmune cholangitis. HEPATOLOGY 2009;49:545-552.
39) **Kawata K**, **Tsuda M**, Yang GX, Zhang W, Tanaka H, Tsuneyama K, et al. Identification of potential cytokine pathways for therapeutic intervention in murine primary biliary cirrhosis. PloS One 2013;8:e74225.
40) **Sun Y**, **Haapanen K**, **Li B**, Zhang W, Van de Water J, Gershwin ME. Women and primary biliary cirrhosis. Clin Rev Allergy Immunol 2015;48:285-300.
41) Zhang H, Carbone M, Lleo A, Invernizzi P. Geoepidemiology, genetic and environmental risk factors for PBC. Dig Dis 2015; 33(Suppl. 2):94-101.
42) Gershwin ME, Selmi C, Worman HJ, Gold EB, Watnik M, Utts J, et al. Risk factors and comorbidities in primary biliary cirrhosis: a controlled interview-based study of 1032 patients. HEPATOLOGY 2005;42:1194-1202.
43) Smyk DS, Rigopoulou EI, Lleo A, Abeles RD, Mavropoulos A, Billinis C, et al. Immunopathogenesis of primary biliary cirrhosis: an old wives' tale. Immun Ageing 2011;8:12.
44) **Bao M**, **Yang Y**, Jun HS, Yoon JW. Molecular mechanisms for gender differences in susceptibility to T cell-mediated autoimmune diabetes in nonobese diabetic mice. J Immunol 2002; 168:5369-5375.

Author names in bold designate shared co-first authorship.

Supporting Information

Additional Supporting Information may be found at onlinelibrary.wiley.com/doi/10.1002/hep.28641/suppinfo.